

Skewness of Atmospheric Flow Associated with a Wobbling Jetstream

University of Reading

Department of Mathematics, Meteorology and Physics

Fay Luxford

August 2010

Supervised by: Dr. Tim Woollings

This dissertation is submitted to the Department of Mathematics and Meteorology in partial fulfilment of the requirements for the degree of MSc Mathematical and Numerical Modelling of the Atmosphere and Oceans.

Abstract

The aim of this dissertation is to investigate the skewness of Z_{250} and Z_{850} . Then to see how much of this skewness can be attributed to shifts in the jet stream north and south, and whether this mechanism can generate skewness values of a comparable magnitude to those observed. These results will be used to estimate how large a role non-linear dynamics play in generating climate atmospheric flow statistics.

Unfiltered observations of geopotential height covering the summer and winter 1958-2001, were used to calculate the skewness. A simple computer model produced a geopotential height profile from a wind profile which combines a jet stream and a synoptic wind noise term. The skewness of the model geopotential heights was then graphed against the skewness of the average observed geopotential heights of the corresponding sector that the model represents.

The observations show positive skewness of the geopotential heights polewards of the mean jet streams and negative skewness equatorwards. The model showed a wobbling jet stream reproduces this pattern, but creates skewness of a larger magnitude. The model showed that when the jet is strong, shifts in it are a major contributor to the skewness pattern and suggests that the basic pattern of skewness can be recreated with linear dynamics.

A limitation of this study is that it only looked at the average of a 30° sector in which the jet winds are strongest. Whether the jet stream plays as large a role in creating the skewness when the winds are weaker has not been investigated. This study found that the strongest gradients in skewness are upstream of the mean strongest jet winds. To understand this, further study in to which characteristics of the jet stream create the most skewness could be undertaken.

Acknowledgements

I would like to acknowledge my supervisor Tim Woollings who has been very helpful, patient and kind. I would also like to acknowledge the financial support of the Natural Environmental Research Council (NERC) without whom this year would not have been possible. Finally I would like to thank my family for their continuing support.

Declaration

I confirm that this is my own work, and the use of all material from other sources has been properly and fully acknowledged.

Signed..... Date.....

Contents

1	Introduction	5
2	Methodology	11
2.1	Data	11
2.2	Skewness of the Observed Geopotential Heights	12
2.3	Basic Model	13
2.4	Parameters	15
2.5	Updated model	18
3	Analysis	20
3.1	Skewness of the Observed Geopotential Heights	20
3.1.1	Skewness of Z_{250}	20
3.1.2	Skewness of Z_{850}	22
3.1.3	Discussion of the Skewness of the Z_{250} and the Z_{850} and Possible Explanations	23
3.2	Updated Model	26
3.3	Limitations of the Methodology	30
4	Conclusions	36
A	ERA-40 Atlas: Climatological Winds	39

Chapter 1

Introduction

Several studies have found that geopotential height is positively skewed on the poleward side of the midlatitude jetstream and negatively skewed on the equatorward side (White, 1980; Trenberth and Mo, 1985; Nakamura and Wallace, 1991).

Skewness is a measure of the of asymmetry of a probability distribution. If a distribution has a longer tail to the left of the mean, then the distribution is negatively skewed. If a distribution has a longer tail to the right of the mean, then the distribution is positively skewed. A Gaussian distribution has zero skewness. The k^{th} statistical moment about the mean is

$$m_k = \sum_{i=1}^n \frac{(x_i - \bar{x})^k}{n} \quad (1.1)$$

where x_i is the i^{th} observation, \bar{x} is the sample mean and n is the number of observations in the sample. The sample skewness is the measure of skewness used in this study, the equation for it is

$$s = \frac{m_3}{m_2^{3/2}}. \quad (1.2)$$

White (1980) calculated the geographical distribution of skewness (the third statistical moment about the mean) of unfiltered geopotential heights recorded over 12 summers (1966 to 1977) and 11 winters (1965-66 to 1975-

76), in the Northern Hemisphere. He found statistically significant negative skewness over the low latitude oceans at 1000 hPa. At 500 hPa statistically significant positive skewness was found north of the climatological mean jet stream and negative skewness south.

Trenberth and Mo (1985) followed up White's (1980) study by investigating geopotential height anomalies at 500 hPa and 1000hPa in the Southern Hemisphere (10-90°S). They looked at daily height fields in both summer and winter using data from May 1972 to November 1980. They found that there was strong evidence for the frequency distribution of height anomalies to be skewed, with positive skewness polewards of the polar jet stream and negative skewness equatorwards. These findings agree with those of White (1980) found in the Northern Hemisphere; however in the Southern Hemisphere the dividing line is at higher latitudes 50-60°S. The most statistically significantly skewed region was found to be 30-45°S. In this region the largest skewness values were generally in the Eastern Hemisphere, north of the polar jet stream.

Nakamura and Wallace (1991) examined 6-day lowpass filtered Z_{500} and sea-level pressure anomalies in the Northern Hemisphere (north of 20°N) for 30 winters (1955-84). Generally they found positive skewness north of the mean stormtrack latitudes and negative skewness south of them for Z_{500} . For the sea-level pressure field they found the skewness pattern to be weaker, especially at high latitudes and with a bias towards negative skewness. At 500 hPa the pole-equator contrast was found to be particularly pronounced around the Pacific and Atlantic stormtracks. They classed the Atlantic stormtrack to be 80-20°W and the Pacific stormtrack to be 140°E-140°W. They investigated whether the skewness pattern changed when the stormtracks moved or were stronger/weaker than their climatological average. They found the distribution of skewness over the Atlantic and (less clearly) over the Pacific was sensitive to changes in the stormtracks. The skewness pattern moved north and south with the stormtrack and was more pronounced when the stormtrack was more intense. When the stormtracks move so do the jet streams.

This observed skewness pattern is usually interpreted as being caused by cut-off lows on the equatorward side of the jet and cut-off highs on the poleward side (Trenberth and Mo, 1985; Nakamura and Wallace, 1991). However it seems likely that much of the observed skewness may arise due to simple, even linear, shifts of the jet to the north and south. The jet represents a strong gradient in geopotential height. So for example the geopotential height at a point on the northern side of the mean jet location will be affected much more when the jet moves north than when the jet moves south. The aim of this project is to investigate this theory and determine if this mechanism can generate skewness values as large as those observed. Skewness which is the result of shifts in the jet stream, has already been observed in association with ocean jets (Hughes *et al.*, 2009). Relevant literature which attempts to explain the observed skewness pattern is discussed below.

White (1980) identifies a connection between the skewness pattern and the jet stream and also a connection between the skewness and regions of blocking. He found a strong link between skewness and extreme values of geopotential height and he found the maximum values of geopotential height (for both 500 hPa and 1000 hPa) occurred in the eastern portions of ocean, in regions of blocking. He also noted that the strongest gradients in skewness (over the Pacific and the Atlantic) occur in roughly the same position as the mean position of the two major jet streams, although they are downstream from the jet maxima in both summer and winter.

Nakamura and Wallace (1991) suggest as a possible explanation, that blocking anticyclones in high latitudes and cutoff lows in lower latitudes are the dominant contributor to the observed skewness pattern. Trenberth and Mo (1985) also suggest they play a role in skewing the frequency distribution. Nakamura and Wallace (1991) put forward this idea on the basis that the skewness pattern shows large meridional contrast across the climatological-mean stormtracks. Quantities such as temperature and potential vorticity also exhibit large meridional contrast across

the climatological-mean stormtracks, this is why the air is often thought of as being two separate masses, a warm mass equatorwards and a cool mass polewards, meeting at the same latitudes as the stormtracks and being mixed together by baroclinic waves along the boundary. Blocking anticyclones are thought of as an isolated vortex of warmer air that has become cut-off from the rest of the warmer air flow. With associated flow anomalies acting against the mean flow advection, this vortex can remain stationary for a relatively long time, giving higher than average geopotential heights over the region it covers. Vice-versa, cut-off lows are colder air that becomes cut off from the cooler air flow and give lower than average geopotential heights. Infrequent and of large amplitude, these events would fit the observed statistics, since Nakamura and Wallace (1991) found that 'large-amplitude anomalies that occur less than 5% of the time are responsible for virtually all the skewness'. They do not make any attempt to prove that cutoff flow configurations create the observed skewness pattern. They do attempt to prove a connection between the distribution of skewness and the position and strength of the stormtracks, as previously mentioned. The position of the jetstream and the stormtracks is very similar (Woollings, 2010). Hence their finding: a connection between the distribution of skewness and the position and intensity of the stormtracks supports the theory that the skewness is caused by the jet wobbling, equally as well as it supports the theory that the skewness pattern is due to cutoff flow configurations. They dismiss the idea that the skewness is directly related to the jetstreams on the basis that the mean strongest winds in the jet streams occur upstream of the regions of strongest skewness of geopotential height.

Holzer (1996) spatially filtered geopotential height fields throughout the troposphere and found the skewness to be small in the tropics and polar regions and large and negative in zonal bands approximately centred on the climatological jet position. This skewness pattern contradicts what was found in other studies (White, 1980; Trenberth and Mo, 1985), although Nakamura and Wallace (1991) did find a bias towards negative skewness at 1000hPa. Donohoe and Battisti (2009) warn that spatially filtering data introduces major biases into the statistics when tracking sea level pres-

sure features or geopotential at mid and upper levels putting in to doubt Holzer's findings. Holzer (1996) surmised that the large negative skewness was caused by advective non-linearity in the balance equation, however he only clearly identified this as the cause for the filtered winds. If the observations do show a bias towards negative skewness around the jet stream, it will be considered that the pattern could arise from a combination of even skewness around the jet due to the jet wobbling, and general negative skewness due to advective non-linearity in the balance equation, as suggested by Holzer. His model used a Gaussian wind profile that is obviously unrealistic and he did suggest that asymmetry in the flow itself could be responsible for the remaining positive skewness.

In conclusion, recent papers (White, 1980; Trenberth and Mo, 1985; Nakamura and Wallace, 1991) have found that most of the skewness comes from occasional extreme values. Nakamura and Wallace (1991) and Trenberth and Mo (1985) both suggest the extreme values may come from cut-off flow configurations. This idea is supported by White (1980) that found the maximum geopotential heights were found in regions of blocking. These papers also found a link between the jet stream and the skewness pattern: the strongest skewness gradients are in the same position as the jet streams, although downstream of the jet maxima. Nakamura and Wallace (1991) found changes in the skewness pattern corresponded with the timing of changes in the stormtracks.

The equations of motion which describe atmospheric circulation are highly nonlinear, yet simple linear statistical models are often surprisingly skillful at reproducing the statistics of the observed flow. One aspect of the atmospheric circulation which many of these models have been unable to simulate is the skewness, or asymmetry of flow variables, and so this is often taken as an indication that the skewness is the result of nonlinear dynamics. However in 2008 Sardeshmukh and Sura (2009) found linear stochastically forced models, which have correlated additive (state-independent) and multiplicative (state-dependent) noise forcing, can produce certain types of non-Gaussian statistics including skewness. Their findings break the bond

between skewness and nonlinear dynamics: if models can create skewness without nonlinear dynamics, then the skewness need not be a product of nonlinear dynamics.

The aim of this project is to identify how much the wobbling of the jet stream contributes to the observed skewness pattern. Whilst previous studies have analysed the observations and suggested blocking as a feasible explanation, they have not modeled blocking and analysed how much skewness this produces. The modelling approach produces evidence that the effect produces the observations. Thus this project will begin by creating a wind profile (at one longitude and across all latitudes of a hemisphere) which will contain a physically realistic jet. From this wind profile a corresponding geopotential height profile will be created. The model will run for 1000s of days thus giving a distribution of geopotential height at each latitude. The skewness of these distributions can then be compared to the observed skewness. The exact number of days the model will be run for will be determined by testing the model. It needs to be run for as many days as it takes for the wind to become roughly symmetrically skewed about the mean jet peak latitude.

Non-linear dynamics are very important for weather forecasting however it is unknown how large a role they play in producing the observed climate statistics. Skewness has often been used as evidence that non-linear dynamics are important. However if the jet stream is responsible for a large proportion of the observed skewness then models can produce close approximations of the geopotential height statistics using just linear dynamics. Linear models are preferable as they are computationally cheaper and much quicker to run.

In the next chapter the models used in this project are described. In chapter 3 the observed skewness pattern is discussed and then the geopotential height skewness produced from the model jet stream is compared to the observed skewness. Chapter 4 concludes the project.

Chapter 2

Methodology

2.1 Data

The data used for this study comes from the ECMWF ERA-40 reanalysis, 1958-2001. Unless otherwise stated this project uses the westerly wind velocities. The data is daily and on a grid of 80 latitudes by 160 longitudes which cover the whole globe. Data from two seasons has been used: season one: December, January and February (no leap days) and season two: June July and August. i.e. in the northern hemisphere winter and summer and in the southern hemisphere summer and winter. The wind values are unfiltered.

Later in this study the standard deviation of the southerly winds is required. This was also calculated using data from the ECMWF ERA-40 reanalysis, however this time only data from 1996-2001. The North Atlantic Oscillation (NAO) is a climatic phenomena of fluctuations in the difference between sea level pressure at the Icelandic low and Azores high. The period 1996-2001 was chosen because NAO varies positive and negative in this timescale, giving a range of NAO affected values. The southerly wind values were recorded on the same 80 latitude by 160 longitude grid but this time 6 hourly measurements were used. Pre-calculated 2-6 day band-pass filtered southerly winds were available and used. They were filtered using Lanczos filtering as described by Duchon (1979). This method of filtering was used to significantly reduce Gibbs oscillations. Donohoe and

Battisti (2009) found for tracking sea level pressure features that temporal filtering has minor problems but spatial filtering launches major biases into the statistics. They found the problem was equally bad when tracking geopotential in the middle atmosphere and even worse when tracking geopotential at upper levels. Thus to reduce bias only data that has been temporally filtered and not spatially filtered was used.

2.2 Skewness of the Observed Geopotential Heights

Previous studies have used smaller data sets than are available in this study and have focused on just one hemisphere. Therefore this study will recalculate the skewness from the raw data, to give enhanced confidence in any skewness pattern that is found and also to allow for an unbiased comparison of the skewness patterns in the two hemispheres to be made. The skewness pattern in each hemisphere will now be calculated from data sets covering the same time period.

The skewness will be calculated at each point on the 160 longitude by 80 latitude grid, for both summer and winter. Previous studies have mainly concentrated on the skewness of the geopotential height at 1000 hPa and 500 hPa, however this study will look at the skewness at 850 hPa and 250 hPa. The subtropical jet is mostly confined to the upper troposphere whereas the eddy-driven jet extends throughout the height of the troposphere (Woollings *et al.*, 2010). Thus at 250 hPa the effect of both jets can be observed and at 850 hPa the effect of just the eddy-driven jet can be observed.

The updated model will produce a graph of the skewness in geopotential height over all latitudes of a hemisphere and at one longitude. Due to the parameters entered into the model, this longitude will be representative of the average of a 30 °S sector. Therefore the skewness of the observed geopotential heights over the same 30 °S sectors will also be calculated for comparison with the model output.

2.3 Basic Model

To look at the effect of the jet on geopotential height, firstly a kinematic model of a jet stream with a simple Gaussian profile was created. It is based on the equations for one in Monahan and Fyfe (2006). At each time step (one time step equals one day) this model gives a value of the wind at each latitude which is the average wind over all longitudes. In this model only the jet winds are present. The equation for the wind is

$$u(\phi, t) = U(t) \exp\left(\frac{-[\phi - \Phi(t)]^2}{2\sigma^2(t)}\right) \quad (2.1)$$

where $U(t)$, $\Phi(t)$ and $\sigma(t)$ are the jet strength, position and width respectively.

$$U(t) = U_0 + \xi(t) \quad (2.2)$$

$$\Phi(t) = \phi_0 + \lambda(t) \quad (2.3)$$

$$\sigma^{-1}(t) = \sigma_0^{-1}[1 + \eta(t)] \quad (2.4)$$

In the above U_0 is the time mean jet peak velocity, ϕ_0 is the time-mean jet central latitude and σ_0^{-1} is the inverse time-mean jet width. The fluctuations in the jet peak velocity and central latitude are $\xi(t)$ and $\lambda(t)$ respectively and the scaled fluctuations in inverse jet width is $\eta(t)$. The fluctuations $\xi(t)$, $\lambda(t)$ and $\eta(t)$ are Gaussian time series with mean zero i.e.

$$p(\xi) = \frac{1}{\sqrt{2\pi\gamma^2}} \exp\left(\frac{-\xi^2}{2\gamma^2}\right) \quad (2.5)$$

$$p(\lambda) = \frac{1}{\sqrt{2\pi\omega^2}} \exp\left(\frac{-\lambda^2}{2\omega^2}\right) \quad (2.6)$$

$$p(\eta) = \frac{1}{\sqrt{2\pi\nu^2}} \exp\left(\frac{-\eta^2}{2\nu^2}\right) \quad (2.7)$$

where γ , ω and ν are the standard deviations of ξ , λ and η respectively. Note from equation (2.4) that this model allows σ to become negative, however if ν is sufficiently small the probability of a negative width is negligible. This must be kept in mind later when the parameters are differed from those given by Monahan and Fyfe (2006), especially as wind velocities

will be averaged over a smaller range of longitudes and thus the standard deviation may increase.

Following Monahan and Fyfe (2006), to preserve the observed correlation between strength and inverse width the program sets $\xi(t) = \rho\nu(t) + \varepsilon(t)$ and again, as in Monahan and Fyfe (2006), the small residual ε has been neglected. Fyfe and Lorenz (2005) found jet strength and position to be linearly uncorrelated thus $\xi(t) = \rho\nu(t)$ will be used in conjunction with 2.3 and 2.4 to find the strength, position and width.

Latitude and width fluctuations are calculated using an AR1 process as follows. For latitude and width fluctuations there is a lag-1 correlation (r_l and r_w respectively) between the current value and the one on the previous day. Using the properties of the bivariate normal distribution (Wilks, 1995) the current fluctuation comes from a conditional Gaussian distribution. A random number from this conditional distribution can be generated using the following formulae.

$$\lambda(t) = r_l\lambda(t-1) + \omega n_1\sqrt{1-r_l^2} \quad (2.8)$$

$$\eta(t) = r_w\eta(t-1) + \nu n_2\sqrt{1-r_w^2} \quad (2.9)$$

where n_1 and n_2 are two independent random numbers from a standard Gaussian distribution.

Secondly the model turns this wind profile into a geopotential height profile. The ageostrophic component of the wind is being ignored and it is assumed that the wind is equal to the geostrophic wind i.e. $u = u_g$. The equation connecting the geostrophic wind and geopotential height is

$$f u_g = -g \frac{dZ}{d\phi} \quad (2.10)$$

where $f = 2\Omega \sin(\phi)$ is the Coriolis force, ϕ is the latitude, Ω is the earths rotation rate, u_g is the geostrophic wind, g is the gravitational constant and Z is geopotential height (Vallis, 2009). Integrating this gives

$$2\Omega \int_a^b \sin(\phi) u_g d\phi = -g[Z]_a^b \quad (2.11)$$

This project will only consider winds above the surface boundary layer. Here the wind is a good approximation of the geostrophic wind: the true wind should be within 10% of the geostrophic wind. Thus the wind profile has been directly substituted for the geostrophic wind profile. Equation (2.11) can be estimated as

$$2\Omega \sin\left(\frac{a+b}{2}\right) u_g \left(\frac{a+b}{2}\right) d\phi \approx -g[Z_b - Z_a] \quad (2.12)$$

Hence

$$Z_b = Z_a - \frac{2\Omega \sin\left(\frac{a+b}{2}\right) u_g \left(\frac{a+b}{2}\right) d\phi}{g} \quad (2.13)$$

This is the basic model and to begin with it was run for the Southern Hemisphere winter (May-September) 500hPa zonal mean zonal wind. The following best fit parameters from Monahan and Fyfe (2006) were used: $U_0 = 23.3 \text{ ms}^{-1}$, $\gamma = 2.7 \text{ ms}^{-1}$, $\phi_0 = -47.5 \text{ degree (deg)}$, $w = 2.7 \text{ (deg)}$, $\sigma_0^{-1} = 0.095 \text{ deg}^{-1}$, $\nu = 0.165$ and $\rho = 13.1 \text{ ms}^{-1}$ and the approximation $Z_{equator} = 5700 \text{ m}$. Geostrophic wind is calculated at 1° intervals. Under the approximation that the radius of the earth is constant, $d\phi$ is also constant, the value at 45° has been used i.e. $d\phi = 111132 \text{ m}$. Since Z_{500} is a lot less than the radius of the earth $g=9.8$ has been used. As can be seen from equation (2.13) wind velocity and geopotential height are on a staggered grid, with geopotential height being measured at 1° intervals from the equator 0° to the pole -90° and wind velocity being computed every 1° from -0.5° to -89.5° .

2.4 Parameters

The updated version of the basic model will produce a 250hPa and a 850hPa geopotential height field for both hemispheres in the winter and summer. To create these fields new parameters need to be found to enter into the

model. These new parameters are derived from the ECMWF ERA40 re-analysis, giving confidence that the patterns observed in the model data have been generated realistically and could occur in the real atmosphere. To confirm that the model can produce realistic values, randomly chosen observed wind profiles were entered, then using them the model produced corresponding geopotential height profiles. The model geopotential height profiles were compared to the observed profiles. In general it was found that the model geopotential heights were within 10% of the observed geopotential heights. This broke down most frequently in the 20° near the pole. In this region the model produced values which were up to 20% larger than the observed values. In this project an error of up to 10% is deemed acceptable. This method of generating geopotential heights from a wind profile will be used in the project. However when drawing conclusions from the results, the fact that this method decreases in accuracy around the pole will be taken in to account.

Monahan and Fyfe (2006) give a Gaussian Jet fitting Procedure, which given a positive wind profile at one longitude, can fit a Gaussian Jet, returning the width and the jet-peak velocity and latitude of this jet.

As discussed in the introduction the skewness pattern is strongest where the jet stream is strongest. Hence firstly the effect of the jet on skewness at the latitude where the jet is strongest will be investigated: it is most likely a pattern will be observed here. The Monahan and Fyfe (2006) model averaged the winds over all longitudes. In this project the winds will be averaged over a 30 degree sector instead. The sectors have been chosen firstly on the basis of where the jet winds are strongest in the given season, hemisphere and pressure level, using the ECMWF ERA-40 Atlas. Secondly the skewness of the observed geopotential height at these longitudes was then checked. Sectors which deviated largely from the simple positive skewness polewards of the jet and negative skewness equatorwards of the jet were replaced with the next strongest wind sector that did have this skewness pattern.

The average wind over a 30° sector was entered into the jet fitting procedure instead of the wind at one longitude to reduce the noise, as the data is not filtered. The model selects the highest value from the averaged winds and then selects all the values around this until it gets to a negative value, which it then ignores and stops. This is done to separate the jet from the rest of the wind, so the fitting can be used. Unfortunately the fitting does not work on every day. For example days when the wind is positive at most latitudes and the jet is in a highly uncentral position produce unphysical results and thus were ignored.

After the jet fitting procedure has been applied, the values for the width and the jet peak latitude and velocity that it provides are screened through another program, to remove the data from days where the fitting has not worked. To ensure the jet remains physically realistic, the program will ignore the data from a day if any of the following occur: the width of the jet exceeds 90° , the jet peak latitude is greater than 90° or less than -90° and if the jet peak velocity exceeds 80ms^{-1} at 850 hPa or 200ms^{-1} at 250 hPa. The jet fitting procedure involves taking the inverse of a matrix and for wind profiles which are highly non-Gaussian this can lead to a single or almost single matrix which creates unrealistic values, days on which this occur are also ignored, as our days when the fitting produces a jet with a complex width. The jet fitting procedure fails less than 6% of the time. Table 2.1 shows for each scenario, the number of days ignored. It also shows the percentage of the data that is ignored.

The jet fitting procedure determined the width of the jet on each day, giving a distribution of width from which the mean and standard deviation were found. As mentioned in section 2.3 to avoid the model jet having a negative width ν must be $O(10^{-1})$. The standard deviation of the scaled fluctuations in the inverse jet width is what ν represents. In this project ν is set equal to the inverse of the standard deviation of the width distribution. Using this estimation, the observations gave $0.1 < \nu < 0.4$. Monahan and Fyfe used $\nu = 0.165$ and deemed this sufficiently small that the model jet width would always be positive. Thus the new values of ν are also suf-

Pressure	Hemisphere	Months	No ° of Days Ignored	% of Days Ignored
250	Northern	DJF	42	0.95
250	Northern	JJA	180	3.99
250	Southern	DJF	8	0.18
250	Southern	JJA	103	2.28
850	Northern	DJF	103	2.34
850	Northern	JJA	245	5.43
850	Southern	DJF	20	0.45
850	Southern	JJA	35	0.78

Table 2.1: The number of days that were not used to calculate the parameters and the percentage of all the days used that they represent.

ficiently small and so the width of the model jet is always positive.

The jet width and jet-peak velocity and latitude are computed for each day of the data. The mean and standard deviation of these distributions are then computed and these values are the parameters used in the model.

2.5 Updated model

The basic model produced physically realistic results, but the skewness was too extreme at latitudes far from the average jet latitude. To overcome this a synoptic noise term will be added when computing the wind velocity at each time step. The synoptic noise value will be a random number from a Gaussian distribution with mean zero and the same standard deviation as the southerly winds for the corresponding hemisphere and season. The distributions of the synoptic noise with the largest (in red) and smallest (in blue) standard deviations are shown in figure (2.1).

There is always the same mass of air between the earth's surface and a pressure surface thus the average geopotential height should be the same at each timestep. In the original model the value of geopotential height at the equator was constant. In the updated version the value at the equator will be modified at each time step to ensure conservation of mass.

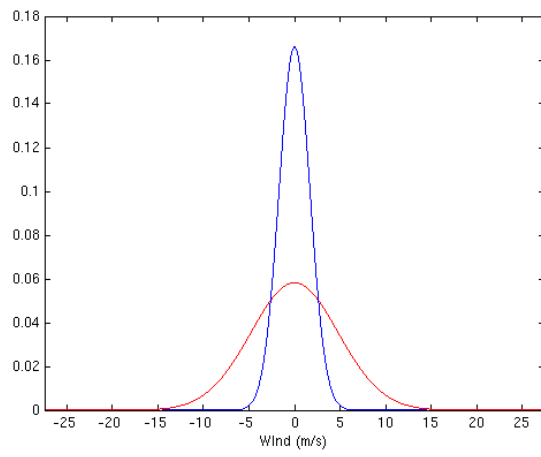


Figure 2.1: Synoptic Wind Noise Distributions with the Largest (red) and Smallest (blue) Standard Deviations

Chapter 3

Analysis

To begin with, the skewness of the observations is examined for patterns and to identify regions with large values of skewness. The results are graphed and compared to the findings of previous studies. Next the skewness of a 30° longitudinal section is compared to the updated model skewness for this section. The two are graphed together and the findings discussed. Finally, potential errors and problems with the model, the data and their implications are outlined.

3.1 Skewness of the Observed Geopotential Heights

3.1.1 Skewness of Z_{250}

The skewness of 250 hPa geopotential height observations has been calculated for the months December, January and February (DJF) and also June, July and August (JJA). The results are shown in Figure (3.1).

In each hemisphere and in each season the same basic skewness pattern can be observed: positive skewness around the pole; a ring of zero skewness at roughly the same latitude as the mean peak latitude of the jet stream; equatorwards a large annulus of negative skewness; another ring of zero skewness; at lower latitudes, approaching the equator, sometimes a full, sometimes a partial annulus of positive skewness which is thinner than the

negative annulus. This agrees with the earlier findings of White (1980) and Trenberth and Mo (1985) who at 500 hPa found positive skewness at high latitudes and negative skewness south of the mean jet stream.

The gradients of skewness are strongest in the Northern Hemisphere. Similar to the findings of White (1980) and Nakamura and Wallace (1991) on different pressure surfaces, in the Northern Hemisphere winter (DJF) the most extreme values of skewness occur over the Pacific and Atlantic jet streams, the Pacific being stronger. For both hemispheres in DJF the strongest skewness gradients are upwind of the jet maxima. However this is not a consistent pattern. In the Southern Hemisphere winter (JJA) the winds over and east of Australia are distinctively stronger than the rest of the jet, yet upstream of this (over Africa) the gradient is at its weakest. The jet is fairly continuous in the Northern Hemisphere summer (JJA) and the magnitude of skewness is continuously large. The highest values of skewness occur in general over oceans although this is not true for the Northern Hemisphere summer (JJA). Knowledge of the climatological winds was gained from the ERA-40 atlas and the graphs used can be found in appendix A.

The Northern Hemisphere summer (JJA) stands out as having the strongest skewness values: it follows the basic pattern described above, however the maximum positive skewness near the pole is 0.3 whereas in the negative annulus it is around -1.5. This is the largest contrast in magnitude between the two regions. In contrast to the other scenarios, the location of the climatological jet peak winds is not in the zero skewness region, but near it on the edge of the negatively skewed region. The skewness near the equator is up to 0.3 which is comparable with the other scenarios.

The basic pattern of skewness is not so clear in the graph of the Southern Hemisphere winter (JJA). Negative gradients are very strong as the skewness decreases rapidly over a short distance whereas positive ones are weaker as they increase over a larger distance. This pattern is mirrored in the winds and is due to a split in the jet stream near New Zealand. The

climatological mean jet stream has a steep gradient equatorwards changing from its maximum over central Australia to around $5ms^{-1}$ at the northern edge of Australia, whereas the wind doesn't fall to $5ms^{-1}$ to the south of the peak until the edge of Antarctica.

3.1.2 Skewness of Z_{850}

Following the calculations of the skewness of Z_{250} , the skewness of the 850 hPa geopotential height observations has been calculated for the same months December, January and February (DJF) and also June, July and August (JJA). The results are shown in Figure (3.2).

The basic pattern observed at 250 hPa, breaks down at 850 hPa. Overall there is a clear bias towards negative skewness. The lowest value of skewness is just less than -1.8; in contrast the highest value is less than 0.5. For the Southern Hemisphere (both seasons) and the Northern Hemisphere winter (DJF) the pattern does resemble the basic pattern described above. However the region of positive skewness near the pole is much smaller, fragmented and of a lower magnitude. The negative skewness covers most of the hemisphere. In the area around the equator the skewness is generally zero, though there are some positive patches and in other places the negative annulus expands right to the equator.

In the Northern Hemisphere there is strong negative skewness south of the Pacific and Atlantic jets. The mean jet peak latitude is in the negatively skewed region too. In the Southern Hemisphere (JJA) the region of zero skewness does roughly correspond to the mean position of the jet and there is increasing negative skewness south of this. Above Antarctica there is a region of positive skewness and a region of negative skewness. As seen at 250 hPa, the Northern Hemisphere summer (JJA) stands out as different. Even the less distinctive pattern described above and seen in the other Z_{850} scenarios breaks down here. Most of the hemisphere is covered by negative skewness. Near the equator skewness is generally zero and occasionally positive. There is a region of positive skewness over the Middle East with a tail that stretches east. From the ERA-40 climatological winds

it can be seen that the strongest jet is over the Arabian Sea. North of this jet is a region of positive skewness and South of it is a region of negative skewness. The maximum skewness in this positive region and the minimum value in this negative region are of equal magnitude (about 0.4).

Previous studies have looked at the skewness of Z_{1000} and Z_{500} rather than Z_{850} and Z_{250} . But, as in this study, for the higher pressure level Nakamura and Wallace (1991) found the pattern to be less clearly related to the stormtracks (their study only investigates the Northern Hemisphere). White (1980), also using unfiltered winds, found negative skewness to cover most of the Northern Hemisphere at 1000 hPa however Nakamura and Wallace (1991) using filtered winds, found much less negative skewness.

3.1.3 Discussion of the Skewness of the Z_{250} and the Z_{850} and Possible Explanations

In summary computation of the Skewness of the unfiltered Z_{250} and Z_{850} found in the Northern Hemisphere positive skewness north of the Subtropical jet stream and negative skewness south. Similarly, in the Southern Hemisphere there is positive skewness south of the Polar jet stream and negative skewness north of it. The results show a bias towards negative skewness which is stronger at 850 hPa and also at 250 hPa in the Northern Hemisphere summer (JJA).

The skewness has been calculated from unfiltered geopotential heights. Previous studies have shown a bias towards negative skewness in unfiltered values which is not present in 6-day lowpass filtered values (White, 1990; Nakamura and Wallace, 1991). As suggested by Nakamura and Wallace (1991) this bias towards negative skewness is likely to be a ‘reflection of the asymmetry inherent in the gradient wind equation: the high-frequency fluctuations associated with migrating cyclones tend to be of shorter duration and more intense than those associated with anticyclones.’ If this is the case, it is unclear why is it stronger at 850 hPa and at 250 hPa in the Northern Hemisphere summer. Perhaps it is because the jet stream is

weakest in the Northern Hemisphere summer and storms have a stronger effect on geopotential height in the lower troposphere.

This study wishes to find how much the wobbling of the jet stream contributes to the skewness pattern. It is expected that the wobbling will create positive skewness polewards of the mean jet position and negative skewness equatorwards, as described earlier. In the next section the model will test whether a wobbling jet stream can produce this skewness pattern and if so, of what magnitude. However for now the previous figures will be analysed with the assumption that it does and see if they are consistent with this idea. In general I believe they are. At 250 hPa the pattern is clear: there is zero skewness at the position of the mean jet peak, positive skewness polewards and negative skewness equatorwards. At 250 hPa in the Northern Hemisphere summer (JJA) and generally at 850 hPa the whole pattern has a bias towards negative skewness, but the pattern remains consistent with a positive/negative skewness pattern created by the jet plus a bias towards negative skewness.

Nakamura and Wallace (1991) and White (1980) both dismissed the idea that the skewness pattern was the product of movements in the jet stream because the strongest skewness gradients occurred downstream of the mean jet maximum. I would also expect the maximum gradient in the skewness to occur at the same location as the maximum gradient in the wind. The results of this study agree with the previous papers: in DJF at 250 hPa this is not the case. However at 250 hPa in the Southern Hemisphere winter (JJA) the strongest gradient in the skewness is in the same place as the strongest gradient in the wind. Some of the data does support the idea that the skewness pattern is the result of the jet stream's movement, however clearly if it is true then the difference in location in DJF would need to be explained.

In the Southern Hemisphere winter (JJA) at 250 hPa, the skewness pattern shows a steep negative gradient in contrast to a shallower positive gradient. The same pattern is mirrored in the winds of the jet. The fact

that the jet pattern is reproduced in the skewness pattern is a good indicator that the jet is responsible for creating the skewness.

The pattern of the skewness of Z_{850} in the Northern Hemisphere summer (JJA) is the least uniform. The ERA-40 Atlas shows that the corresponding winds are also much less uniform. There is not a continuous subtropical jet, rather there are lots of jets of very similar strength covering most of the oceans. There is one jet that is significantly stronger than the others over the Arabian Sea. It was mentioned earlier that the skewness pattern is very clear around it. This almost symmetric pattern of skewness is exactly the pattern as it is thought a wobbling jet would create.

The expected pattern is less clear at 850 hPa compared to at 250 hPa. At 850 hPa the subtropical and polar jet are also less clearly defined as there are more regions of strong winds. Due to the close proximity and comparable strength of other jets that are not present in the upper troposphere it is hard to distinguish the effect of a single wobbling jet in the lower troposphere, which is what this project wishes to do. For example at 850 hPa in the Southern Hemisphere winter (JJA) the polar jet contains the strongest winds, which are creating the general positive skewness near the pole and negative skewness in the midlatitudes pattern. However there are other strong winds over Antarctica: here the basic model would assume positive skewness but there is in fact a positive region and a negative one.

As explained in the introduction the observed skewness pattern is usually interpreted as being caused by blocking. Below the distribution of blocking as found in other studies is compared to the skewness distribution calculated in this study.

Trenberth and Mo (1985) found at 1000 hPa and 500 hPa in the Southern Hemisphere that the primary location for blocking events is the New Zealand sector of the hemisphere, the second maximum occurs south east of South America and there is a weak maximum in the Indian Ocean. Skewness of geopotential height is also strong in the New Zealand sector.

However the largest magnitude values of skewness around South America occur on the South West side not the South East. Over the Indian Ocean is another region with high values of skewness of geopotential height. Trenberth and Mo (1985) found this to be a weak maximum of blocking at 1000 hPa and even weaker at 500 hPa whereas at 850 hPa in the summer (DJF) this is one of the two regions containing the highest magnitude of skewness.

Tyrlis and Hoskins (2008) identified the primary region of blocking in the Northern Hemisphere to be the Eastern Atlantic Ocean through Europe and in to central Asia. They found the second region of maximum blocking to be the Central and Eastern Pacific Ocean. At 250 hPa in the summer (JJA) the latitudinal profile of skewness is similar at all longitudes. In the other scenarios a large gradient in the skewness was found across the Central and Eastern Pacific which correlates with the region of high blocking. However Tyrlis and Hoskins (2008) also found blocking to be very infrequent over western parts of the Pacific basin, yet at 850 hPa in the summer (JJA) this is the location of the strongest skewness gradient. Also they found in July and August maximum blocking occurred in eastern Europe and Asia, yet skewness in this region is small at Z_{850} (at Z_{250} the gradient is uniformly strong around the hemisphere and this region does not stand out).

In conclusion, due to inconsistencies in location and relative strength, this study weakens the case for blocking being the primary cause of the observed skewness of geopotential height.

3.2 Updated Model

The graphs in Figures (3.3) and (3.4) show the skewness of the observed geopotential height from a 30° sector (in green) plotted against the skewness of the model geopotential heights (in red). For reference, the line of zero skewness and a line through the mean peak jet latitude (both in blue) have been added. The longitudes of the 30° sectors are shown in table

(3.1).

Pressure	Hemisphere	Months	Longitudes (°)
250	Northern	DJF	119.25 - 150.75
250	Northern	JJA	279.00 - 310.50
250	Southern	DJF	0.00 - 29.25
250	Southern	JJA	119.25 - 150.75
850	Northern	DJF	159.75 - 189.00
850	Northern	JJA	299.25 - 330.75
850	Southern	DJF	60.75 - 90.00
850	Southern	JJA	49.50 - 81.00

Table 3.1: The longitudes of the 30 ° sectors used

The model clearly shows that the wobbling jet stream creates positively skewed geopotential heights polewards and negatively skewed geopotential heights equatorwards of its position. In general the shape of the curve which represents the skewness of the observations is well replicated by the shape of the model curve. This is less true further from the mean jet peak latitude. Reasons for this are discussed below. Whilst the model manages to capture the general shape, the magnitude of the model skewness is significantly larger than that of the observations. The model curve is smoother than the observation curve: this is to be expected as this curve represents the skewness of values from 10 000 days, whereas the observational data covers around 4000 days.

In most of the situations the model skewness is zero at the mean jet peak latitude. Where it is not, the difference is only a couple of degrees. Given enough observations it would be expected that the mean jet peak latitude (of a Gaussian jet) would be the location of zero skewness. This implies that the model data set is too short. The model runs for 10 000 days, where as the observations cover roughly 4000 days. Therefore caution should be taken in drawing too much from small differences between the observed latitude of zero skewness and mean peak jet latitude, as the difference may be because the data set is too short. The jet fitting proce-

dure used to gain the mean jet peak latitude, attempts to fit a Gaussian jet profile to the physical jet profile. If the physical jet profile is not Gaussian then even with enough observations to fully represent the distribution, the mean peak jet latitude may not actually represent the location of zero skewness.

The shape of the model curve best replicates the shape of the observed curve near the mean jet peak latitude. Given the design of model it is not surprising that it is less accurate further from the mean jet. The model produces jet winds plus a background noise term, so at high or low latitude a lot of the time the wind values mainly come from the random background noise term. During testing it was found that the error in the models method for producing geopotential height from the wind velocity doubled from 10% to 20% between 70° to 90° in the Northern Hemisphere and -70° to -90° in the Southern Hemisphere.

The model was run for 10 000 days so ensure the skewness of the model winds were roughly symmetric about the mean jet peak latitude (ignoring regions too far from the mean jet peak position). The maximum and minimum values of the skewness of geopotential height in each scenario are generally within 0.5 of each other. Some of this variation will be from the synoptic wind noise term in the model wind equation. At 250 hPa in the Northern Hemisphere winter (DJF), the winds are symmetrically skewed in the range 5-65 degrees, but in the same range the maximum positive skewness of geopotential height is almost 2.5 and the minimum is above -1. As well as the variation added by the synoptic wind noise term, the difference may be caused by the equation for geopotential height, which emphasises gradients in the wind near the pole. Generally the difference between the model maximum and minimum is relatively small compared to the magnitude of the skewness. Looking at the observations of the Northern Hemisphere summer (JJA) at both 250 hPa and 850 hPa and the Southern Hemisphere (both hemispheres) at 850 hPa the magnitude of negative skewness is larger than that of positive skewness and at the mean peak jet latitude the skewness is negative. This suggests a bias towards neg-

ative skewness, as was seen in the skewness maps of the whole hemispheres.

Ignoring the 20° near the poles the model curves of the skewness of Z_{250} in both hemisphere in DJF fit the shape of the skewness of the observed geopotential heights very well, although as mentioned above the model pattern is asymmetric in the Northern Hemisphere.

At first glance the graph of the skewness of Z_{250} in the Southern Hemisphere winter (JJA) shows the worst fit between the model and the observations. Concentrating on the region around the mean jet peak latitude, in the other scenarios there is one positive region of skewness polewards of roughly the mean jet peak latitude and one region of negative skewness which starts roughly equatorwards of the mean jet peak latitude, similar to the pattern of skewness created by the model. In this scenario there are two peaks in positive skewness, each followed by a section of negative skewness north of them. South of the mean jet peak latitude the model skewness is positive; the observed skewness goes from positive to negative. Then north of the mean jet peak latitude the model skewness is negative; the observed skewness again goes from positive to negative. To understand it better we need to recall the pattern noticed previously when looking at the skewness of the whole hemisphere. In the previous section it was noted that for this scenario the jet winds were asymmetric (the jet in fact has split in two), the skewness pattern duplicated the same asymmetry. The model was given the mean peak jet latitude and other parameters which it used to create a symmetric jet. Because the physical jet wind profile is very skewed the mean jet peak latitude does not correspond to the latitude where the strongest winds occur. Figure (3.5) shows the graph again, but a vertical line has been added at approximately the latitude where the ERA-40 atlas shows the strongest winds in the jet are. Polewards of this line you can see the skewness is predominately positive and equatorwards it is predominately negative. From 0° to around -10° is being ignored as at these latitudes the pattern is unlikely to be a product of the jet. So the model skewness and the skewness of the observations do show the same positive polewards, negative equatorwards pattern but because the

observed geopotential heights have been affected by an asymmetric jet and the model comes from a symmetric jet, the latitudes at which the skewness changes from positive to negative are out of sync. The jets asymmetry is also reproduced in the skewness of the observations: positive skewness covers a larger range of latitudes than negative skewness. In contrast the model is much more symmetric.

The graph of the skewness of Z_{850} in the Northern Hemisphere winter (DJF) shows that both the model and observations have larger magnitude negative skewness than positive. The general pattern of positive skewness north of the mean jet peak latitude and negative skewness south is in both and as expected the model shows this pattern more smoothly. The latitude at which the skewness is zero for the observations occurs roughly 7° south of the mean peak jet latitude. In the other 850 hPa scenarios there is a negative bias: at the mean jet peak latitude the skewness is negative, but here the skewness is positive.

The model skewness is considerably larger than that of the observed geopotential heights. This is probably due to the simplicity of the model, as it only represents one jet plus a background wind noise term. The results suggest that other processes that are not represented in the model but are in the raw observations act to reduce the skewness. At 850 hPa the climatological wind graphs show there is more than one jet and thus the observed pattern is actually the result of them interacting. Also Rossby waves are not represented in the model.

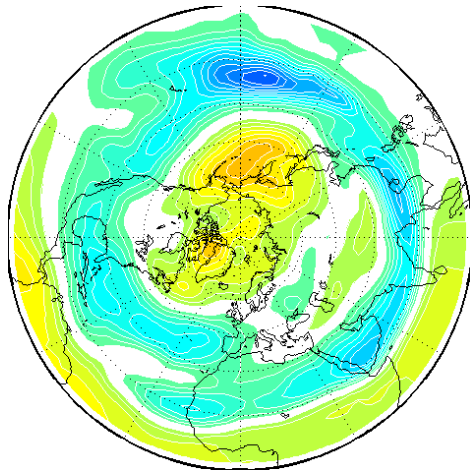
3.3 Limitations of the Methodology

One limitation is that the model can only ever have one jet. Previous research has shown there is often more than one jet (e.g. Woollings *et al.*, 2010). The model results may more closely represent observations if the model contained two or even three jets as Woollings *et al.* (2010) implies there is. Another limitation of the model is it does not cap the jet, hence sometimes it goes unrealistically close to the pole or the equator.

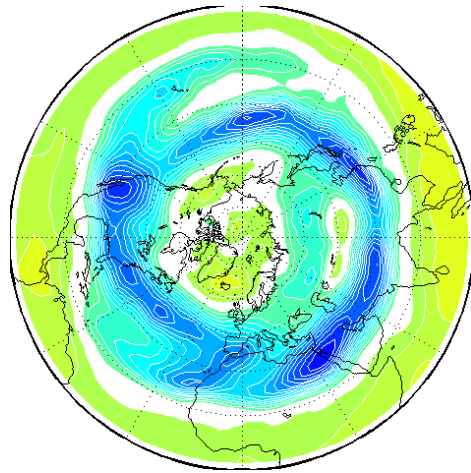
The way the model wind profile is converted into a geopotential height profile will also lead to errors, as it is not exact. Firstly it assumes the wind is the geostrophic wind and in testing, when it was used to turn observed wind profiles into geopotential height profiles, these had an error of up to 10% which increased to 20% in the 20° near the pole.

The model represents the average of a 30° sector in which the winds are their strongest. It is then assumed that whatever skewness of geopotential heights the jet causes in this sector is similarly caused in other sectors, but the magnitude of the skewness will be smaller in the same proportions as the difference in the jet winds. However in sections where the jet is weak, it may be that other factors are the primary cause of the skewness of the geopotential heights.

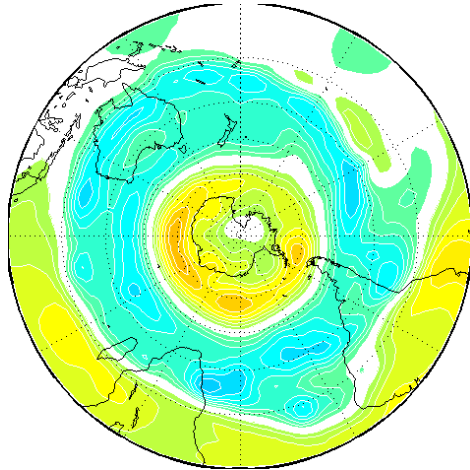
Finally the observed winds are averaged over the 30° sector before the jet fitting procedure is applied. The isotachs are not always parallel to the lines of latitude. When they are not, the averaging process will distort the wind distribution which may make the jet created by the jet fitting procedure unrepresentative of the observed jet. The difference between the angle of the isotachs and the lines of latitude is not generally large thus hopefully this has not created a large error. In fact the only time it is large is for the jet going up the Arabian Sea at 850 hPa in the Northern Hemisphere summer (JJA) but the 30° sector chosen for this scenario did not include this jet.



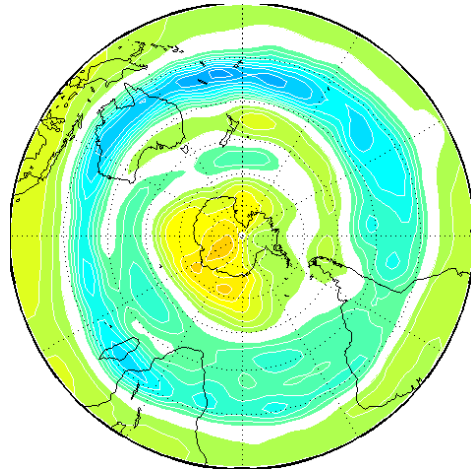
(a) Northern Hemisphere DJF



(b) Northern Hemisphere JJA

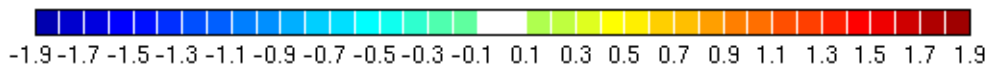


(c) Southern Hemisphere DJF



(d) Southern Hemisphere JJA

Skewness



(e) Key

Figure 3.1: Skewness of Z_{250}

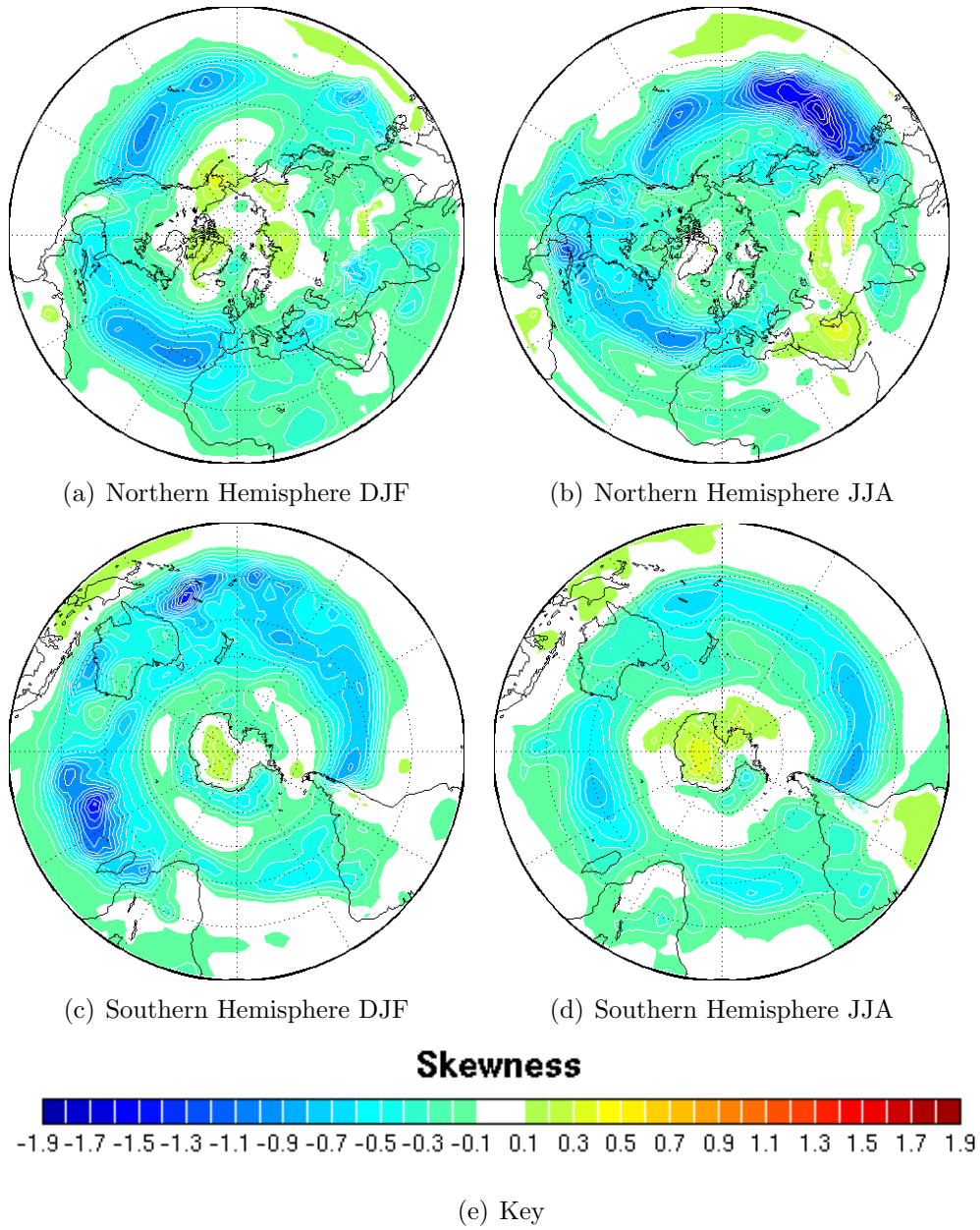


Figure 3.2: Skewness of Z_{850}

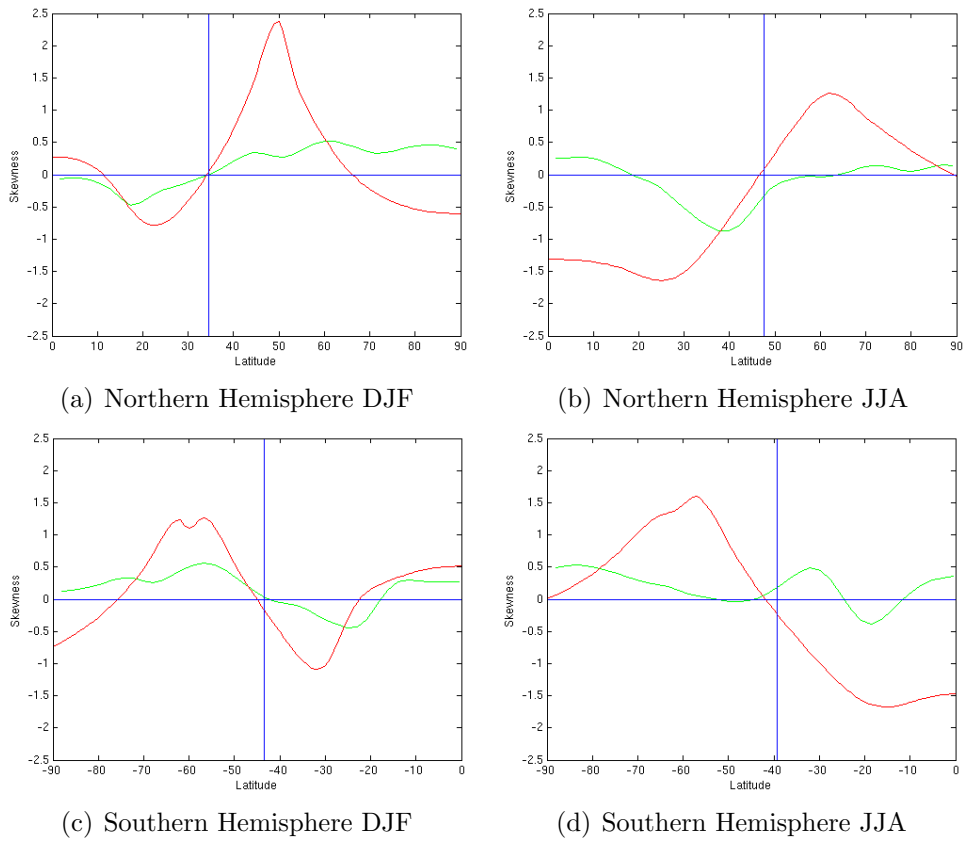


Figure 3.3: Model (red) and Observed (green) Skewness of Z_{250}

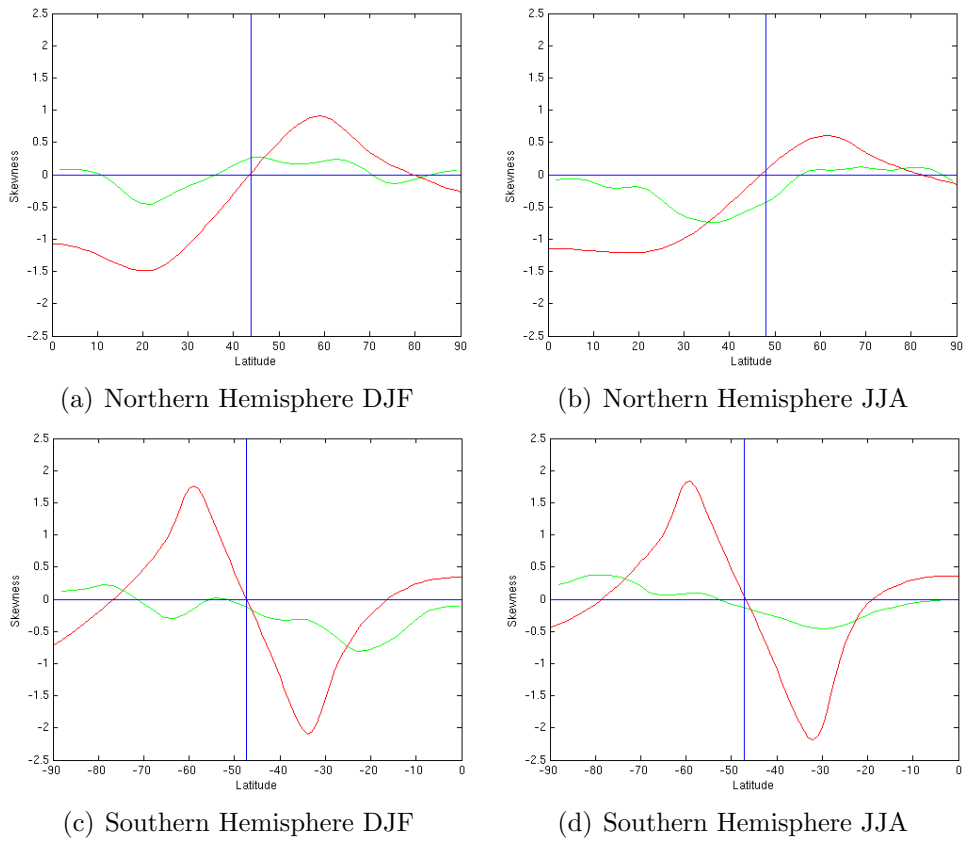


Figure 3.4: Model (red) and Observed (green) Skewness of Z_{850}

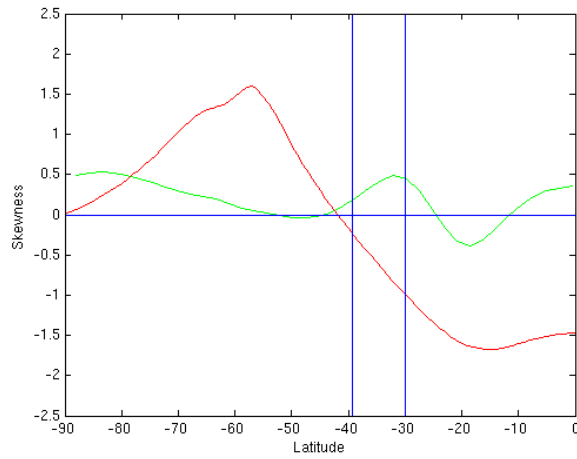


Figure 3.5: Model (red) and Observed (green) Skewness of Z_{250} in the Southern Hemisphere JJA

Chapter 4

Conclusions

Previous studies have found that geopotential height is positively skewed on the poleward side of the jet stream and negatively skewed on the equatorwards side. The aim of this project was firstly to recalculate the skewness using a larger data set and at different pressure levels, to check this pattern was present. Secondly to investigate how much of the skewness was caused by simple shifts in the jet stream north and south, and to see if this mechanism can generate skewness values as large as those observed. Linear models have previously struggled to reproduce skewed statistics, leading many to take this as evidence that the skewness is the product of non linear dynamics. However Sardeshmukh and Sura (2009) have found it was possible to reproduce skewness with a linear model with stochastic noise. By looking at how much skewness shifts in the jet stream create, this project wishes to discover whether models need the non linear dynamics to be able to create the correct climate statistics of the geopotential height distribution.

The skewness of Z_{250} clearly shows the pattern previously observed. With the exception of the Northern Hemisphere summer (JJA) the skewness of Z_{850} also displays this pattern but with a bias towards negative skewness. The skewness of Z_{850} in the Northern Hemisphere summer (JJA) is mainly negative although around the strongest mean jet, which goes up the Arabian Sea, there is positive skewness North and negative skewness South. In each of the 30° sections chosen, polewards of the latitude of

the mean strongest winds the geopotential height is positively skewed and equatorwards, negatively skewed. Again several of the scenarios showed a bias towards negative skewness. These were the Northern Hemisphere summer (JJA) at both 250hPa and 850hPa and the Southern Hemisphere (both seasons) at 850 hPa.

The model skewness of geopotential height was positive polewards of the mean jet peak latitude and negative equatorwards, for each scenario. Hence the model showed that shifts in the jet stream north and south do produce this skewness pattern. An aim of this dissertation was to see if the jet stream wobbling could produce skewness as large as the values observed; it was actually found that in each scenario the model produced larger magnitude skewness. The model represents the average over a 30° sector, which was chosen as the climatological jet is strongest in this section. Since in this region the model shows the jet produces a strong skewness pattern, in other sectors where the jet is weaker it is assumed the model would correspondingly produce lower magnitude skewness. This would match with the observations, which are seen to have the strongest skewness gradients in the regions around the jet stream. The model does not produce exactly the same skewness as is observed but this project does show that the basic pattern can be recreated with a simple wobbling jet and does not require non linear dynamics.

The results imply that wobbles in the jet stream are the main cause of the skewness pattern but with other effects clearly dampening the skewness and giving a bias towards negative skewness. However it is unclear why in some scenarios the maximum gradient of skewness occurs downstream of the maximum jet winds. White (1980) and Nakamura and Wallace (1991) both dismissed the jet stream as the cause of the skewness because of this flaw. The model results do not allow the contribution of the jet stream to be ignored, but the cause of this difference needs to be identified. Looking at the mean winds may not be the best approach because they do not include any information on the amount of variability. Further study could investigate which characteristics of the jet stream play the largest role in

creating skewness. For example, which produces more skewness a jet with a higher peak velocity or one with larger variability of the jet peak latitude? This may help explain the difference in location between the mean jet peak winds and the maximum skewness of geopotential heights. Alternatively the basic pattern may be attributed to the jet but something then weights it downstream, for example perhaps blocking. In summary a model of the jet stream could reproduce the basic pattern of skewness but to achieve a more accurate result further study into the causes of the skewness is required.

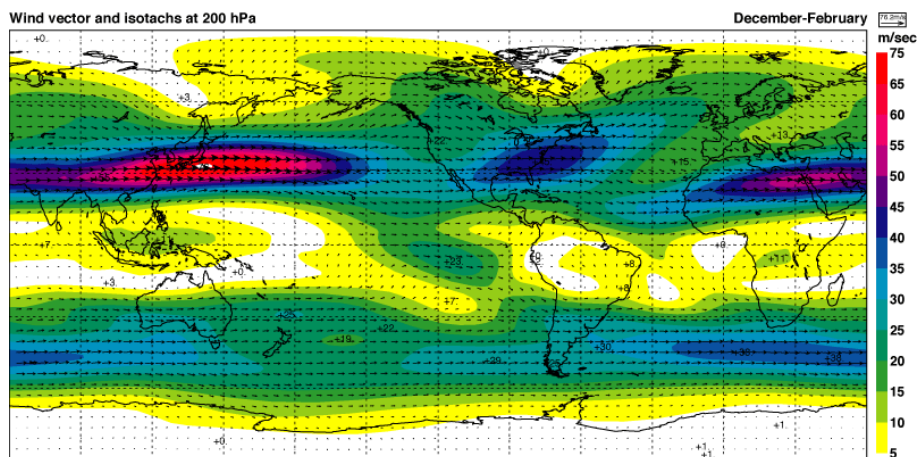
As an extension to this study it would be interesting to know if the model skewness would be closer to the observed skewness if it included more than one jet. The model could also be extended to the whole hemisphere rather than representing the average of a sector.

Several of the papers that investigated the skewness of geopotential height also looked at the kurtosis. It would be of interest to know how much shifts in the jet stream contribute to this pattern and whether the kurtosis can be represented by linear dynamical models.

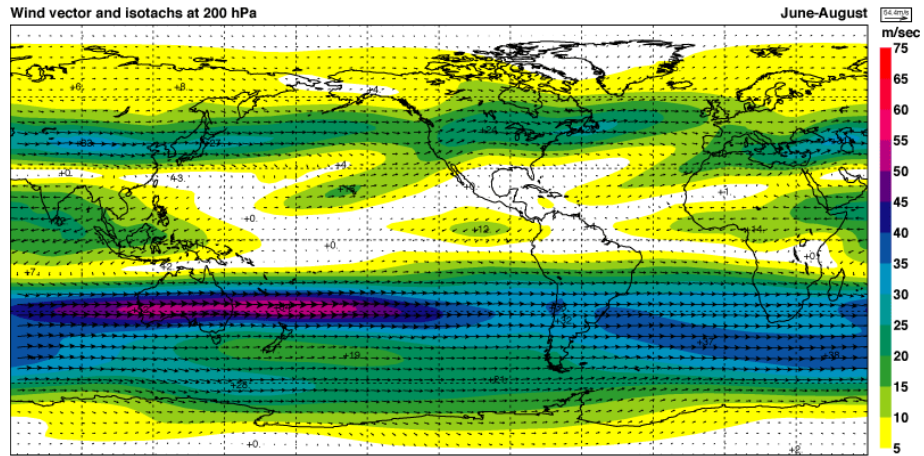
In conclusion the observations show positive skewness of the geopotential heights polewards of the mean jet streams and negative skewness equatorwards. The model showed a wobbling jet stream reproduces this pattern, but creates skewness of a larger magnitude. The model showed that when the jet is strong, shifts in it are a major contributor to the skewness pattern and suggests that the basic pattern of skewness can be recreated with linear dynamics.

Appendix A

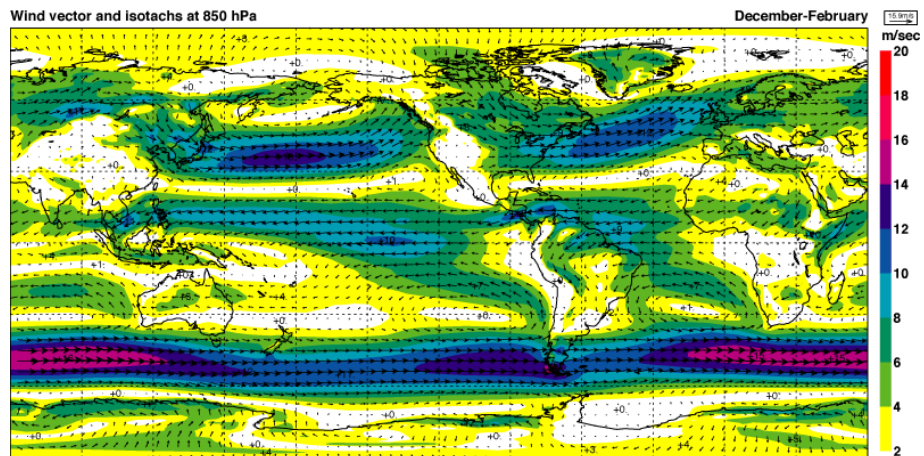
ERA-40 Atlas: Climatological Winds



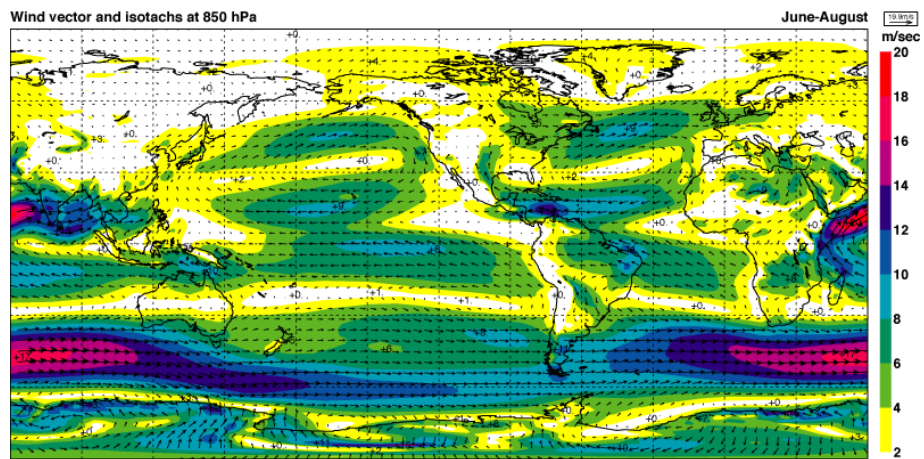
http://www.ecmwf.int/research/era/ERA-40_Atlas/images/full/D01_LL_DJF.gif
[22 July 2010]



http://www.ecmwf.int/research/era/ERA-40_Atlas/images/full/D01_LL_JJA.gif
[22 July 2010]



http://www.ecmwf.int/research/era/ERA-40_Atlas/images/full/D04_LL_DJF.gif
[22 July 2010]



http://www.ecmwf.int/research/era/ERA-40_Atlas/images/full/D04_LL_JJA.gif
[22 July 2010]

Bibliography

- [1] Donohoe, A. and D. S. Battisti, The Amplitude Asymmetry between Synoptic Cyclones and Anticyclones: Implications for Filtering Methods in Feature Tracking. *Mon. Weather Rev.* **137** (2009) 3874-3887
- [2] Duchon, C. E. Lanczos Filtering in One and Two Dimensions. *J. Appl. Meteorol.* **18** (1979) 1016-1022
- [3] Fyfe, J. C. and D. J. Lorenz, Characterizing Midlatitude Jet Variability: Lessons from a Simple GCM. *J. Climate* **18** (2005) 3400-3404
- [4] Holzer, M. Asymmetric Geopotential Height Fluctuations from Symmetric Winds. *J. Atmos. Sci.* **53** (1996) 1361-1379
- [5] Hughes, C. W., A. F. Thompson and C. Wilson, Identification of Jets and Mixing Barriers From Sea Level and Vorticity Measurements using Simple Statistics. *Ocean Model* **32** (2009) 44-57
- [6] Monahan, A. H. and J. C. Fyfe, On the Nature of Zonal Jet EOFs. *J. Climate* **19** (2006) 6409-6424
- [7] Nakamura, H. and J. M. Wallace, Skewness of Low-Frequency Fluctuations in the Tropospheric Circulation during the Northern Hemisphere Winter. *J. Atmos. Sci.* **48** (1991) 1441-1448
- [8] Sardeshmukh, P. D. and P. Sura, Reconciling Non-Gaussian Climate Statistics with Linear Dynamics. *J. Climate* **22** (2009) 1193-1207
- [9] Trenberth, K. E. and K. C. Mo, Blocking in the Southern Hemisphere. *Mon. Weather Rev.* **113** (1985) 3-21
- [10] Tyrlis, E. and B. J. Hoskins, Aspects of a Northern Hemisphere Atmospheric Blocking Climatology. *J. Atmos. Sci.* **65** (2008) 1638-1652
- [11] Vallis, G. K. Atmospheric and Oceanic Fluid Dynamics, *United Kingdom, Cambridge University Press*, 2009.

- [12] White, G. H. Skewness, Kurtosis and Extreme Values of Northern Hemisphere Geopotential Heights. *Mon. Weather Rev.* **108** (1980) 1446-1455
- [13] Wilks, D. S. Statistical Methods in the Atmospheric Sciences, *London, Academic Press*, 1995.
- [14] Woollings, T. Dynamical Influences on European Climate: An Uncertain Future. *Phil. Trans. R. Soc.* **368** (2010) 3722-3756
- [15] Woollings, T., A. Hannachi and B. Hoskins, Variability of the North Atlantic Eddy-Driven Jet Stream. *Q.J.R. Meteorol. Soc.* **136** (2010) 856-868